SPECIAL SECTION PAPER

Switchable polarization volume gratings for augmented reality waveguide displays

Yannanqi Li, SID Student Member | John Semmen, SID Student Member |
Qian Yang, SID Student Member | Shin-Tson Wu, SID Fellow

College of Optics and Photonics, University of Central Florida, Orlando, Florida, USA

Correspondence
Shin-Tson Wu, College of Optics and Photonics, University of Central Florida, Orlando, FL 32816, USA.
Email: swu@creol.ucf.edu

Abstract

A new electrically driven polymer-stabilized polarization volume grating (PVG) is developed. The diffraction efficiency can be modulated by a vertical electric field. A small amount of liquid crystal monomer is doped into the host cholesteric liquid crystal to form a stabilized polymer network to make the unwinding process reversible. The fabricated device exhibits submillisecond response time, a large range of diffraction efficiency modulation, and clear see-through capability. Some potential applications are demonstrated, including a significantly suppressed rainbow effect, enhanced light efficiency, and expanded field of view for a waveguide-based augmented reality display. The unique properties and benefits of switchable PVGs could open a new space in near-eye display research, especially novel optical systems for augmented reality waveguide displays.

KEYWORDS
augmented reality, fast response time, rainbow reduction, switchable gratings, waveguide displays

1 | INTRODUCTION

Augmented reality (AR) headsets have been attracting much attention in recent years. The thin form factor of the diffractive waveguide featuring an eyeglasses-like design stands out among geometrical waveguides and free space AR displays. However, there are still some problems existing in diffractive waveguides, such as low system efficiency, uneven color/brightness uniformity, relatively narrow field of view (FoV), and rainbow effect.[1,2] Currently, three types of input and output couplers are commonly used in diffractive waveguides: surface relief gratings (SRGs), volume holographic gratings (VHGs),[3] and polarization volume gratings (PVGs). Compared to SRGs, PVGs have advantages in lower fabrication cost and higher yield. In comparison with VHGs, PVGs show a larger angular response to support a wider FoV. The PVG

is a slanted self-organized cholesteric liquid crystal (CLC) structure, which induces selective diffraction in wavelength and incident angle.[4,5] Although PVGs have not been adopted into commercial AR products, they are a promising candidate for waveguide couplers.[6–12]

Both passive and active PVGs have been developed; the former uses an LC polymer, and the latter uses an electrically switchable LC material. Passive PVGs have been investigated extensively and integrated into waveguide plates as an input or output coupler to deliver AR images to the user. By designing and optimizing the parameters of a multilayer PVG structure, full-color images with a large FoV can be achieved.[8,9] By contrast, an active PVG employs LC as the switching medium.[13–15] Compared to passive film-type PVGs, active PVGs exhibit two additional features, including dynamic modulation and more LC material selectivity. Here, the dynamic

modulation could be diffraction efficiency modulation, slant angle variation, or grating period change under an external stimulus. The diffraction efficiency modulation offers several advantages to waveguide-based AR headsets, such as improved system efficiency by enabling a dynamic eye-box, expanding FoV with multiplexed PVGs, and reducing the rainbow effect. In terms of commercially available reactive mesogen, to the best of our knowledge, RM257 is the most used LC monomer for spin-coating PVG films. Its birefringence decreases from 0.17 to 0.15 as the wavelength increases from blue to red. In comparison, active PVGs can be realized by many commercial LC materials with birefringence higher than 0.3.

Multistimuli-responsive PVGs can respond to light, temperature, and electric field.[13-15] Among all the external stimuli, electric field is a preferred approach for AR waveguide displays as the LC devices should not be influenced by unintended temperature change or irradiation of an external environmental light. In Chen et al.,[14] a PVG using dual-frequency LC can be electrically switched with different frequencies to tune the diffraction efficiency. A concern of this work is the incomplete reversibility when returning to the initial state after removing the applied electric field.

In this paper, we demonstrate a switchable polymer-stabilized (PS) PVG whose diffraction efficiency can be modulated by a longitudinal electric field. Our fabricated PS-PVG shows an excellent see-through capability and good switching characteristics. We also measured its spectral response and switching time. The spectral response shows that a large diffraction efficiency change can be achieved by the applied voltage. The total response time of the PVG is 0.6 ms at 30 V. In addition, our switchable PVGs dramatically suppress the unwanted rainbow effect, which is a common phenomenon in waveguide-based AR headsets.

2 | WORKING PRINCIPLE

Compared to a planar CLC, PVG presents a slanted structure whose helical axis is tilted with respect to the z axis and the spatially variant LC director orientation in the azimuthal plane, as depicted in Figure 1A. But the PVG still inherits some of the properties of CLC, including polarization-selectivity and LC director reorientation by an electric field (Figure 1B). Especially, the LC director reorientation will decrease the effective birefringence, which in turn leads to transmittance modulation. The CLC structure can be formed easily by doping a positive dielectric anisotropy nematic LC with some chiral dopants. Such a structure will transition to a focal conic state during the relaxation stage when the applied electric field is removed. To achieve a stable switching between the tilted structure and the homeotropic state, a certain amount of LC monomer is doped into the CLC mixture to form a stabilized polymer network, thus making the unwinding process reversible (Figure 1). Such a CLC can relax back to its original tilted state with the aided polymer network.

3 | DEVICE FABRICATION

The basic fabrication process is illustrated in Figure 2A. The PS-PVG was made by sandwiching a thin CLC layer between two ITO (indium tin oxide) glass substrates. First, the glass substrates were cleaned in an ultrasonic cleaner for 8 min. Next, a photo-alignment layer (PAL) was spin-coated onto a cleaned substrate at 800 rpm for 5 s and 3000 rpm for 30 s to create a uniform thin film. Brilliant yellow as our photoalignment material was dissolved in dimethyl-formamide (DMF) solution with a concentration of 0.2% by weight. We used two glass substrates both coated with PAL and assembled them
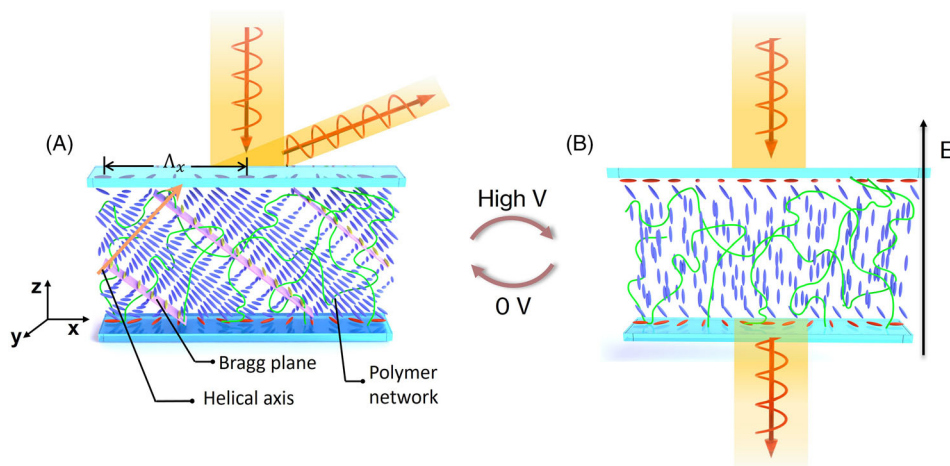
FIGURE 1 Schematic of an electrically switchable PS-PVG under (A) 0 V and (B) high voltage. Green curves indicate the stabilized polymer network. Pink planes indicate the Bragg plane. Orange arrow represents the helical axis. Λ_x is the grating period.
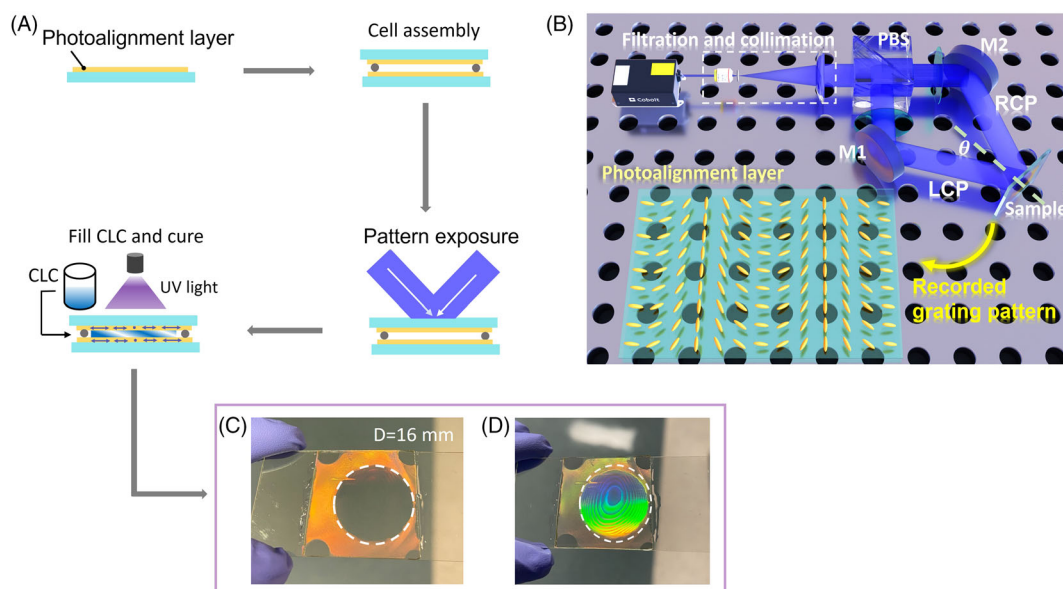
FIGURE 2 (A) Flowchart of fabrication processes for switchable PVGs. (B) Exposure setup. Photos of the fabricated PS-PVG showing (C) see-through capability and (D) diffraction effects at different viewing angles. White dashed lines circle the effective PS-PVG area. PBS, polarization beam splitter; M, Mirror.

together by dispensing a small amount of glue with 4.5 μm silica spacers. The fabricated cell gap is about 3–4 μm across the whole device. Then, the assembled cell was exposed to the interference pattern generated by the polarization interferometry method that is shown in Figure 2B. The photoalignment layer plotted in Figure 2B is magnified for clearly illustrating the exposure grating pattern. Its actual size is 1.6 cm * 1.6 cm. The photoalignment material is a kind of polarization-sensitive azo-dye, which can record the rotating linear polarization pattern of two beam interference between right-handed circularly polarized (RCP) light and left-handed circularly polarized (LCP) light. The interference angle is 34°, yielding a 766-nm grating period. After exposure, the CLC mixture was filled into the cell at 88°C and then cooled down in air to the room temperature (22°C). This annealing process helps to obtain a good CLC alignment. The CLC mixture consists of 90.53% LC host E48 (Merck), 2.32% chiral dopant R5011 (HCCH, China), 7% diacrylate reactive mesogen RM257, and 0.15% photo-initiator Irg819. The last step is to stabilize the PVG structure by polymerization through a high-power UV (~365 nm) LED light. Since the response of PVG is angular dependent, the color appearance of the sample is highly dependent on the viewing angle. The photos of the PS-PVG sample in Figure 2C,D were taken from different angles. Figure 2C shows the high see-through quality of the sample, while Figure 2D shows the sample's appearance when it diffracts light into the user's eye. We noticed the Newton's rings from

the sample in Figure 2D, which is caused by the nonuniformity of the cell gap and the index mismatch between the ITO glass substrate and the LC material. The refractive index of the ITO is ~1.86, while the average index of E48 is ~1.62 in the visible range.

4 | ELECTRO-OPTICAL PERFORMANCE

4.1 | Spectral response

To characterize the spectral response, a collimated white light beam was normally incident on the PVG, and a detector was placed behind to read the transmittance value, as sketched in Figure 3A. To switch the PS-PVG, we applied a 1-kHz alternating rectangular voltage waveform to the cell and recorded the transmittance spectra as Figure 3B depicts. As the applied voltage increases, the LC directors are reoriented toward homeotropic state and the grating effect is gradually reduced, leading to a much higher transmittance. The measured transmittance was calibrated with a nematic LC cell coated with PAL, and the polarization state of the input light was converted to circular. Diffraction efficiency is inferred from the measured transmittance spectra. From Figure 3B, a higher transmittance can be achieved by applying a higher voltage. Our PS-PVG has a lower tolerance to high voltages than commercial cells due to its slightly non-uniform cell gap. Thus, we limited the maximum driving voltage to

FIGURE 3 (A) Sketch of the measurement setup for spectral response to normally incident light. (B) Measured transmittance spectra under different voltages.
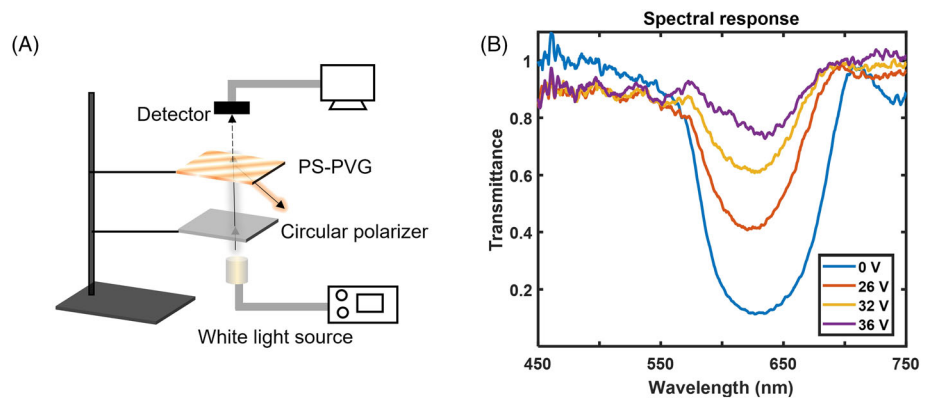
FIGURE 4 (A) Experimental setup for measuring the switching time. (B) Measured time-dependent transmittance curves of the rise and decay cycles.
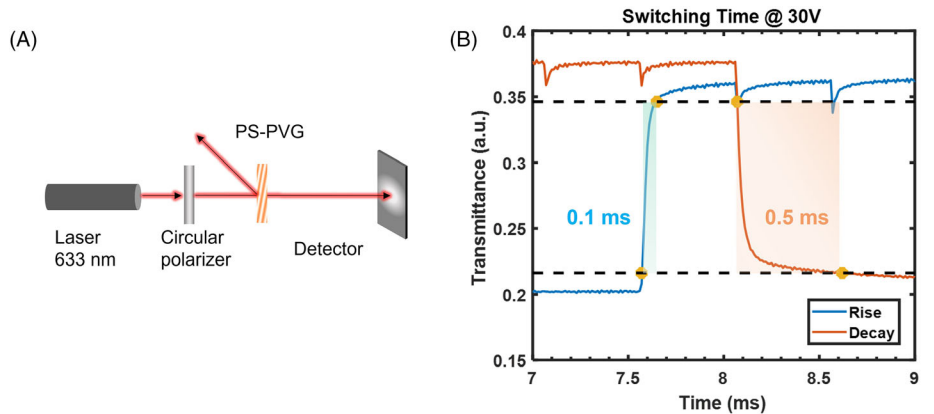
36 V. A more uniform cell will allow for a higher operation voltage, leading to a larger range of diffraction efficiency modulation for the PS-PVG.

4.2 | Switching time

Response time is an important parameter for a switchable device. To characterize the switching time, a detector was placed behind the test cell to record the time-dependent transmittance curves (Figure 4A) when we switched the PS-PVG on and off. Figure 4B shows the measured time-dependent transmittance curves. The total switching time is the sum of rise and decay times which are calculated as the transmittance changes between 90% and 10%. The total switching time is 0.6 ms at 22°C, which is fast enough to enable many applications.

5 | RAINBOW REDUCTION IN WAVEGUIDE

In AR waveguide displays, rainbow is an annoying issue which could interfere the user's viewing experience.[16] Rainbow is a manifestation of color dispersion which is caused by the diffraction of the environmental light by the output couplers. Compared to the transmissive rainbows, the reflective rainbow is more obvious since its environmental light comes from the same side as the display. A k-diagram is presented in Figure 5A to illustrate the interaction between the output grating and environmental light. Two circles are sketched with radii corresponding to the total internal reflection (TIR) angle and grazing angle. After diffraction by the output grating, the k values are distributed in two circles that shift from the origin by the grating k vector. Some diffracted light can enter the see-through FoV and causes the rainbow effect.

There are several ways to reduce the rainbow effect. The most straightforward way is to adopt a higher index substrate, thus requiring a larger grating k vector which will make the shifted circle (yellow circle in Figure 5A) to have a smaller overlapping region with the see-through FoV (purple square in Figure 5A). However, according to calculation, the rainbow effect will not disappear completely until the refractive index of the waveguide substrate exceeds ∼2. Other methods include adding optical filters, optical coating, and optimizing the gratings.

Our proposed switchable PS-PVGs can help mitigate the rainbow effect. When its AR function is used, the PS-PVG can be switched synchronously with the time sequential light engine, like in a liquid-crystal-on-silicon (LCoS) panel.[17] Within the duration of a frame when the
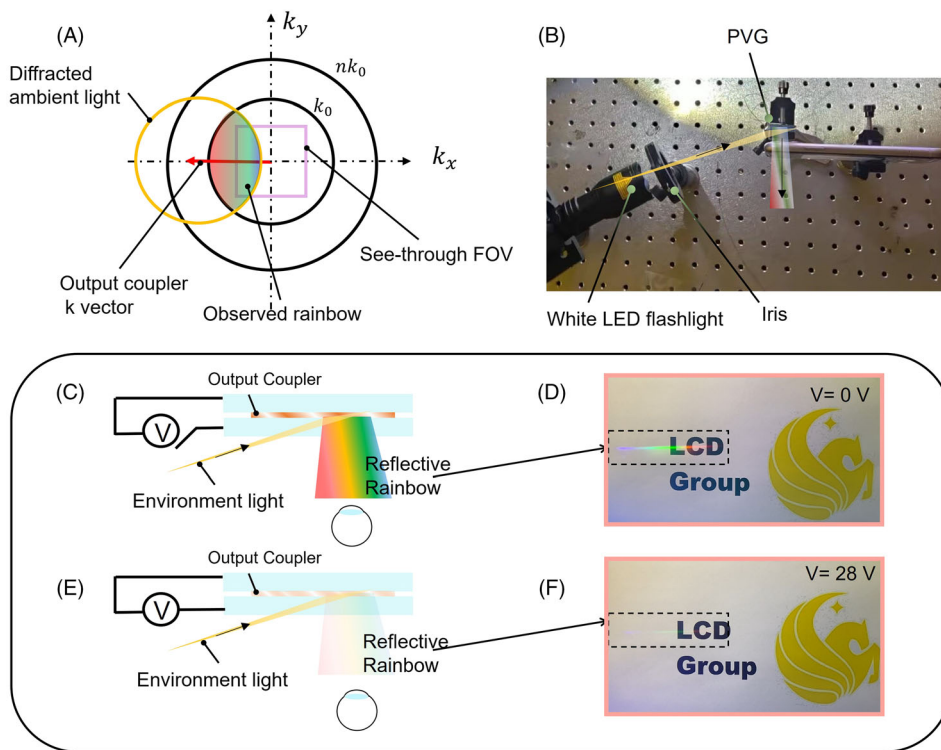
FIGURE 5 (A) Mechanism of the reflective rainbow formation in the two-dimensional k diagram. (B) Photo of measurement setup for rainbow observation. (C) Layout of rainbow formation at 0 V. (D) The appearance of reflected rainbow at 0 V. (E) Layout of rainbow formation at a high V. (F) The appearance of reflected rainbow at a high V.

AR image is on, the PVG should be electrically switched off to deliver the image to user's eyes. When the AR image is off, the PVG can be electrically switched on to reduce rainbow. The synchronization requires a fast-switching time of the output grating. The measured switching time of our PS-PVG ($\sim$0.6 ms) can synchronize with a 240 Hz LCoS display.

Figure 5B shows the experimental setup for rainbow observation. In experiments, we used a white light-emitting diode (LED) flashlight to imitate the environmental light originating from the same side as the viewer. Figure 5C shows the rainbow formation when the output coupler (PS-PVG) is switched off and the rainbow effect can be observed clearly in Figure 5D. When a high voltage is applied to the PS-PVG, the diffraction effect will fade away as the LC directors are reoriented by the electric field toward a homeotropic state. The sketch of rainbow reduction is depicted in Figure 5E. The obvious rainbow reduction effect is ascribed to the high transmittance when the PS-PVG is switched on, indicating that most of the diffraction is vanished. A high see-through image quality of the PS-PVG sample is also validated by the clear view of the printed words and image on a white paper (Figure 5F).

6 | DISCUSSION

A main concern for employing PS-PVGs in practical applications is the operation voltage which is related to the safety and power consumption. In experiment, the applied voltage is up to 36 V, but a lower voltage can be achieved with a more uniform and thinner cell gap. A thinner cell gap requires a lower operation voltage and leads to a faster response time.[18] Although a thinner cell gap will cause a lower diffraction efficiency, it may be beneficial to have a PS-PVG with low diffraction efficiency, such as for use as an output coupler in waveguides for better uniformity in the eye-box.

Besides rainbow reduction, the switchable PVG can also help improve the system efficiency by enabling a dynamic eye-box. Due to pupil expansion, the output light will cover a large eye-box. However, only a portion of the light goes into the user's eyes, which means the rest of the light will be wasted (Figure 6A). With the aid of an eye-tracking apparatus, a dynamic eye-box can be realized by switching off a specific area of the output grating, which corresponds to the user's eye position. Figure 6B,C show a simple sketch of the proposed waveguide configuration enabled by a pixelated PVG. By switching-on the remaining area of the output grating, the light will not be outcoupled until it hits the working area. The extra benefit of this configuration is the increased rainbow reduction and mitigation of the eye glow effect, since only a small part of the grating is working at one time. The density of pixelation of the PVG determines the efficiency improvement. Also, the uniformity of color and brightness should be considered when it comes to practical implementation of the proposed waveguide system.

FIGURE 6   (A) Sketch of a traditional waveguide configuration based on a passive output coupler. (B and C) Sketches of the proposed waveguide configuration with a dynamic eye-box enabled by a pixelated PS-PVG when the pupil is located at different positions.
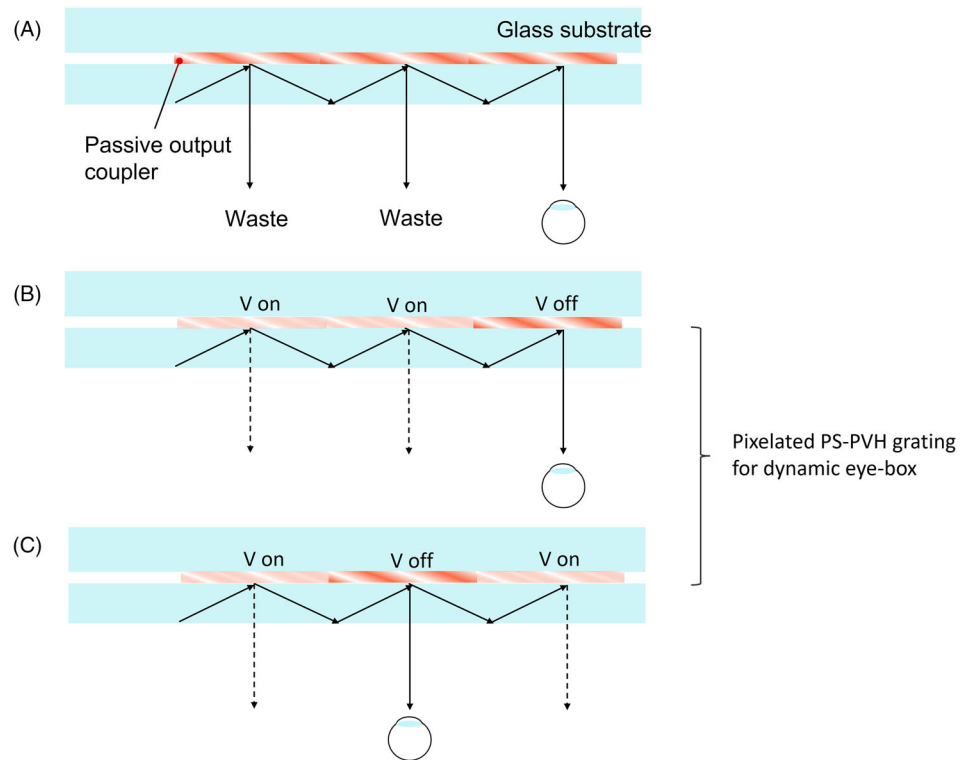
FIGURE 7   (A) Two-dimensional K diagram of double FOV in a waveguide architecture. (B) Simple sketch of a double FOV waveguide structure enabled by two PVGs with different K vectors.
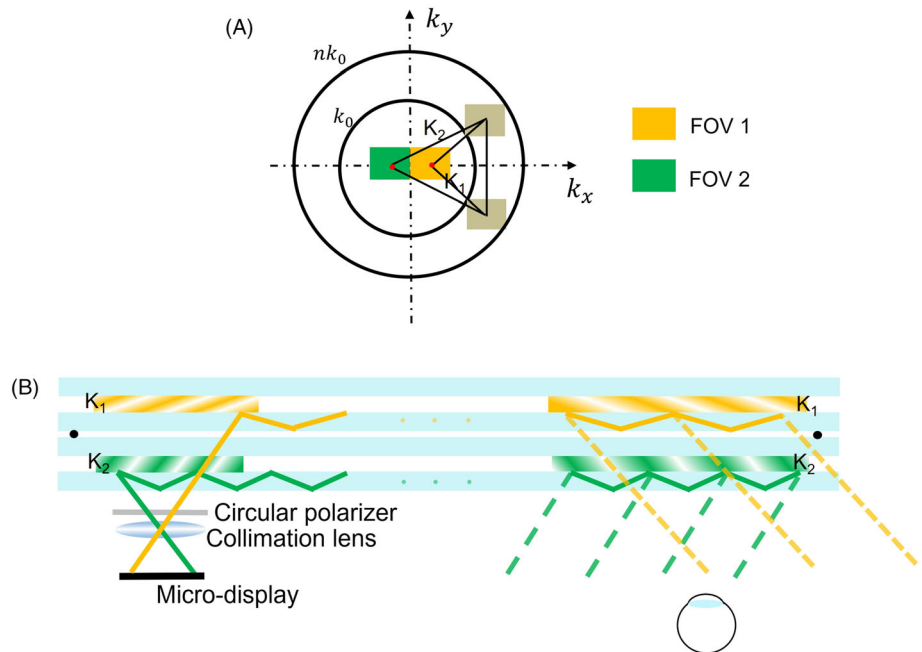
In addition, the FoV can be increased by employing multiplexed PVGs in a time-sequential manner. The supportive maximum range of guiding angles of light in a waveguide is governed by the refractive index of the waveguide plate. As Figure 7A shows, the FOV bounded in the waveguide can be expanded when it is transferred back to air by two PVGs with different k vectors. Each PVG is responsible for each part of the FoV. Figure 7B depicts the waveguide structure with an expanded FoV. It is noteworthy that to avoid the dispersive issue, the net k vector should be zero in one waveguide, which means the k vector value of the input and output coupler should be the same, as noted in Figure 7B. And two waveplates are separated by an air

gap to suppress the crosstalk between two waveguides. The crosstalk we refer here is that, for example, the input light diffracted by the input coupler with K_2 will be guided into the upper waveguide and diffracted by the output coupler with K_1. Such crosstalk will lead to a serious dispersive issue, which can be avoided by the air gap between two waveguides due to TIR. The green and yellow lines represent the chief rays of one single pixel coming from the two edges of a microdisplay panel, respectively. After being coupled and decoupled by the input and output PVG, the stitched FoV will be presented in front of the user's eyes by means of time-multiplexing technology. To achieve full-color performance, multiple waveplates are stacked to cover the display spectrum. To have a good brightness and FoV uniformity, the bandwidth of the light source should be taken into consideration while optimizing the PVG structure.

7 | CONCLUSION

We demonstrate a switchable polymer stabilized PVG with diffraction efficiency modulation for AR waveguide applications. The fabricated PVG exhibits the following properties: (1) a large range of diffraction efficiency modulation, (2) fast switching time (0.6 ms), and (3) high see-through capability. It can be used as the output coupler in AR waveguides to realize the following advantages: (1) reduced rainbow effect (has been demonstrated), (2) dynamic eye-box for improving system efficiency, and (3) doubled FoV with multiplexed PS-PVGs.

ACKNOWLEDGMENT

ORCID
Shin-Tson Wu https://orcid.org/0000-0002-0943-0440

REFERENCES

1. Kress BC. Optical combiners for AR headsets: features and limitations. Proc SPIE 2019;11062:110620J.
2. Cheng D, Wang Q, Liu Y, Chen H, Ni D, Wang X, et al. Design and manufacture AR head-mounted displays: a review and outlook. Light Adv Manuf. 2021;2(3):24. https://doi.org/10.37188/lam.2021.024
3. Sutherland R, Tondiglia V, Natarajan L, Bunning T, Adams W. Electrically switchable volume gratings in polymer-dispersed liquid crystals. Appl Phys Lett. 1994;64(9):1074–76. https://doi.org/10.1063/1.110936
4. Weng Y, Xu D, Zhang Y, Li X, Wu ST. Polarization volume grating with high efficiency and large diffraction angle. Opt Express. 2016;24(16):17746–59. https://doi.org/10.1364/OE.24.017746
5. Zhang S, Chen W, Yu Y, Wang Q, Mu Q, Li S, et al. Twisting structures in liquid crystal polarization gratings and lenses. Crystals. 2021;11(3):243. https://doi.org/10.3390/cryst11030243
6. Li Y, Yang Q, Xiong J, Yin K, Wu ST. 3D displays in augmented and virtual realities with holographic optical elements. Opt Express. 2021;29(26):42696–712. https://doi.org/10.1364/OE.444693
7. Yin K, Hsiang EL, Zou J, Li Y, Yang Z, Yang Q, et al. Advanced liquid crystal devices for augmented reality and virtual reality displays: principles and applications. Light Sci Appl. 2022;11(1):161. https://doi.org/10.1038/s41377-022-00851-3
8. Weng Y, Zhang Y, Cui J, Liu A, Shen Z, Li X, et al. Liquid-crystal-based polarization volume grating applied for full-color waveguide displays. Opt Lett. 2018;43(23):5773–76. https://doi.org/10.1364/OL.43.005773
9. Gu Y, Weng Y, Wei R, Shen Z, Wang C, Zhang L, et al. Holographic waveguide display with large field of view and high light efficiency based on polarized volume holographic grating. IEEE Photonics J. 2022;14(1):7003707. https://doi.org/10.1109/JPHOT.2021.3127547
10. Xiong J, Yang Q, Li Y, Wu ST. Holo-imprinting polarization optics with a reflective liquid crystal hologram template. Light Sci Appl. 2022;11(1):54. https://doi.org/10.1038/s41377-022-00746-3
11. Feng X, Lu L, Yaroshchuk O, Bos P. Closer look at transmissive polarization volume holograms: geometry, physics, and experimental validation. Appl Optics. 2021;60(3):580–92. https://doi.org/10.1364/AO.412589
12. Xiong J, Li Y, Li K, Wu ST. Aberration-free pupil steering Maxwellian display with wide-view broadband polarization converters. J Soc Inf Display. 2021;29(5):298–304. https://doi.org/10.1002/jsid.1010
13. Kobashi J, Yoshida H, Ozaki M. Planar optics with patterned chiral liquid crystals. Nat Photonics. 2016;10(6):389–92. https://doi.org/10.1038/nphoton.2016.66
14. Chen R, Lee YH, Zhan T, Yin K, An Z, Wu ST. Multistimuli-responsive self-organized liquid crystal Bragg gratings. Adv Opt Mater. 2019;7(9):1900101. https://doi.org/10.1002/adom.201900101
15. Chen P, Ma LL, Hu W, Shen ZX, Bisoyi HK, Wu SB, et al. Chirality invertible superstructure mediated active planar optics. Nat Commun. 2019;10(1):2518. https://doi.org/10.1038/s41467-019-10538-w
16. Xiong J, Hsiang EL, He Z, Zhan T, Wu ST. Augmented reality and virtual reality displays: emerging technologies and future perspectives. Light Sci Appl. 2021;10(1):216. https://doi.org/10.1038/s41377-021-00658-8
17. Huang Y, Liao E, Chen R, Wu ST. Liquid-crystal-on-silicon for augmented reality displays. Appl Sci. 2018;8(12):2366. https://doi.org/10.3390/app8122366
18. Li Y, Yang Z, Chen R, Mo L, Li J, Hu M, et al. Submillisecond-response polymer network liquid crystal phase modulators. Polymers. 2020;12(12):2862. https://doi.org/10.3390/polym12122862

AUTHOR BIOGRAPHIES
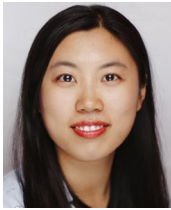
Yannanqi Li received her BS degree in Optics from Sichuan University in 2018 and is currently working toward a PhD degree at the College of Optics and Photonics, University of Central Florida. Her current research interests include novel liquid crystal optical elements and optical system design in AR/VR/3D near-eye displays.

John Semmen received his BS degree from CREOL, the College of Optics and Photonics, University of Central Florida (UCF). He is currently working toward a PhD degree at UCF. His research interests include polarization holography, liquid crystal devices for AR/VR displays, and optical system design.

Qian Yang received his BS degree in Physics from Nanjing University in 2017 and MS degree in Physics from the University of Rochester in 2019. He is currently working toward a PhD degree from the College of Optics and Photonics, University of Central Florida. His current research interests include liquid crystal spatial light modulators for LiDAR applications, planar optics for AR/VR displays, and miniLED and micro-LED displays.

Shin-Tson Wu is a Trustee Chair professor at the College of Optics and Photonics, University of Central Florida (UCF). He is an Academician of Academia Sinica, a Charter Fellow of the National Academy of Inventors, and a Fellow of the IEEE, OSA, SID, and SPIE. He is a recipient of the Optica Edwin H. Land Medal (2022), SPIE Maria Goeppert-Mayer Award (2022), Optica Esther Hoffman Beller Medal (2014), SID Slottow-Owaki Prize (2011), Optica Joseph Fraunhofer Award (2010), SPIE G. G. Stokes Award (2008), and SID Jan Rajchman Prize (2008). In the past, he served as the founding Editor-In-Chief of the Journal of Display Technology, Optica publications council chair and board member, and SID honors and awards committee chair.